Electrochimica Acta 245 (2017) 25–31

Contents lists available at ScienceDirect

Electrochimica Acta

journal homepage: www.elsevier.com/locate/electacta

Self-organized, free-standing TiO_2 nanotube membranes: Effect of surface electrokinetic properties on flow-through membranes

Shiva Mohajernia[a], Anca Mazare[a], Ekaterina Gongadze[b], Veronika Kralj-Iglič[c], Aleš Iglič[b], Patrik Schmuki[a,*]

[a] Department of Materials Science, WW4-LKO, University of Erlangen-Nuremberg, Erlangen, Germany
[b] Laboratory of Biophysics, Faculty of Electrical Engineering, University of Ljubljana, Ljubljana, Slovenia
[c] Laboratory of Clinical Biophysics, Faculty of Health Sciences, University of Ljubljana, Ljubljana, Slovenia

ARTICLE INFO

Article history:
Received 28 April 2017
Received in revised form 16 May 2017
Accepted 17 May 2017
Available online 19 May 2017

Keywords:
TiO_2 nanotube
Membrane
Electrochemical anodization

ABSTRACT

In the present work we investigate the effect of the surface electrokinetic properties and presence of background ions on the flow of a marker dye through TiO_2 nanotube membranes. We believe the results to be of high significance not only for filtration but also for the design of microphotoreactor application based on photoactive TiO_2 nanotubes membrane. First, both-side open, high aspect ratio TiO_2 nanotube membranes were obtained by fast anodization of Ti to self-aligned TiO_2 nanotube layers, followed by a lift-off process. Then we investigated the permeation through the TiO_2 nanotube membranes by diffusion of acid orange 7 (AO7) and extracted the dye diffusion rates. The effects of pH, ionic concentration, and size of ions were investigated, and the results were compared with theoretical modeling of the surface charge of TiO_2 and the neighbouring electric double layer as a function of different species of ions; the modeling confirms the experimental data. We observed a remarkable influence of the background ion species, as well as of ion concentrations and pH in the feed solution on the diffusion rate of AO7. The results of modeling are well in line with the observed influence of TiO_2 nanotube inner surface charge and effective size (hydrodynamic radius) of the ions in the background solution. It is also observed that the absolute permeate flux and the membrane's permeability strongly depend on the electric and wetting conditions of the membrane surface.

1. Introduction

Self-organized TiO_2 nanotube layers grown by electrochemical anodization have over the past years been widely investigated in applications such as photovoltaics, nano-templates, sensors, photocatalysis, etc. [1–10]. One particularly elegant direction towards applications is the use of nanotube layers as lifted-off membranes. Such TiO_2 nanotube membranes have received considerable attention in the last years, due to the combination of their controllable dimensions and crystal structure with unique functional properties [9]. Particularly such membranes can be used in solar cells or filters for size selective exclusion but also as flow through photoreactors [10,11]. Typically lifted-off TiO_2 membranes have individual tube diameters of 50-100 nm and tube lengths in the range of 15-250 μm. Generally, ion or molecule flow through membranes of such dimensions is comparably rare and mainly based on polymeric or Al_2O_3 membranes [12,13]. From these experiments, typically, two parameters are found to have significant effects on the passing through behavior, namely the permeate-pH and the concentration of the species of interest in the feed electrolyte. Changes in these two parameters can facilitate or hamper the permeation or in some cases even cause clogging of the membrane [14].

For TiO_2 based membranes, such studies have not been reported. As the oxide surface is amphoteric and therefore the surface charge density and the net charge vary as a function of pH [15], pH effects need to be particularly considered in view of membrane performance. Therefore, isoelectric point (IEP), i.e. the pH at which the surface carries no net electrical charge, is a crucial parameter. In the absence of other specifically adsorbed ions, tube walls are expected to have a net positive charge below the pH of the IEP and should be negatively charged at higher pH values. Additionally, the membrane surface charge can be altered by

* Corresponding author.
E-mail addresses: shiva.mohajernia@fau.de (S. Mohajernia), anca.mazare@fau.de (A. Mazare), ekaterina.gongadze@fe.uni-lj.si (E. Gongadze), veronika.kralj-iglic@zf.uni-lj.si (V. Kralj-Iglič), Ales.Iglic@fe.uni-lj.si (A. Iglič), schmuki@ww.uni-erlangen.de (P. Schmuki).

http://dx.doi.org/10.1016/j.electacta.2017.05.115
0013-4686/

complexation of the tube/pore walls with ionic species, and such alterations can have a significant effect on the membrane permeability.

There are numerous reports in literature on the effect of pH on the permeate flux through membranes. Hua et al. [16] reported that the permeation of oily waste water through Al_2O_3 membrane was greatest near the pH of 5.8. In addition, Zhang et al. [17] showed an obvious shift in the isoelectric point of Al_2O_3-TiO_2 composite membranes from 8.3 (Al_2O_3 membrane) to 6.1, which results in a stronger negative surface charge on the Al_2O_3-TiO_2 membrane surface and higher permeation. Ionic concentration is the other crucial parameter which has significant effect on permeation. If indicator molecules (dyes) are used, increased salt concentration may also induce the aggregation of charged molecules in the electrolyte solution, and this consequently may alter their osmotic coefficient [18], i.e. aggregates may have considerably larger hydrodynamic radii than the monomers and this greatly influences their self-diffusion coefficient [19].

In the present study, we prepare free standing TiO_2 nanotube membranes and study the effect of pH, electrolyte concentration and size of the ions on the permeation flux of a marker dye (acid orange 7 (AO7)) through the TiO_2 nanotubular membrane and compare the results with quantitative modeling of changes induced on electrical, wetting and hydrodynamic properties.

2. Material and Methods

2.1. Membrane preparation

Highly ordered TiO_2 nanotube arrays were prepared by potentiostatic electrochemical anodization of Ti foils (0.125 mm thick, 99.7% purity, Advent) in a two-electrode electrochemical cell, with a Pt foil as counter electrode and Ti foil as working electrode. Before anodization, the Ti foils were cleaned in acetone, ethanol and deionized water by sonication, and then dried in a N_2 stream. The anodization experiments were performed at 120 V for 10 minutes, in an ethylene glycol-based (EG) electrolyte with 5 wt. % deionized water, 1.5 M Lactic acid and 0.1 M of NH_4F. To establish uniform nanotube geometry, we used a two-step anodization treatment. For producing free standing lift-off tube membranes we followed a simple re-anodization approach [9]: the as-prepared samples were annealed at 250 °C in air for 1 h, this led to a partial crystallization, and then the samples were anodized again at 120 V for 2 minutes to form a second tube layer underneath the crystalline tube array. This underlying amorphous layer can be preferentially dissolved by immersion in H_2O_2 solution, while the crystalline tube layer, being more stable in such an environment, detaches as an entirely self-standing nanotube membrane.

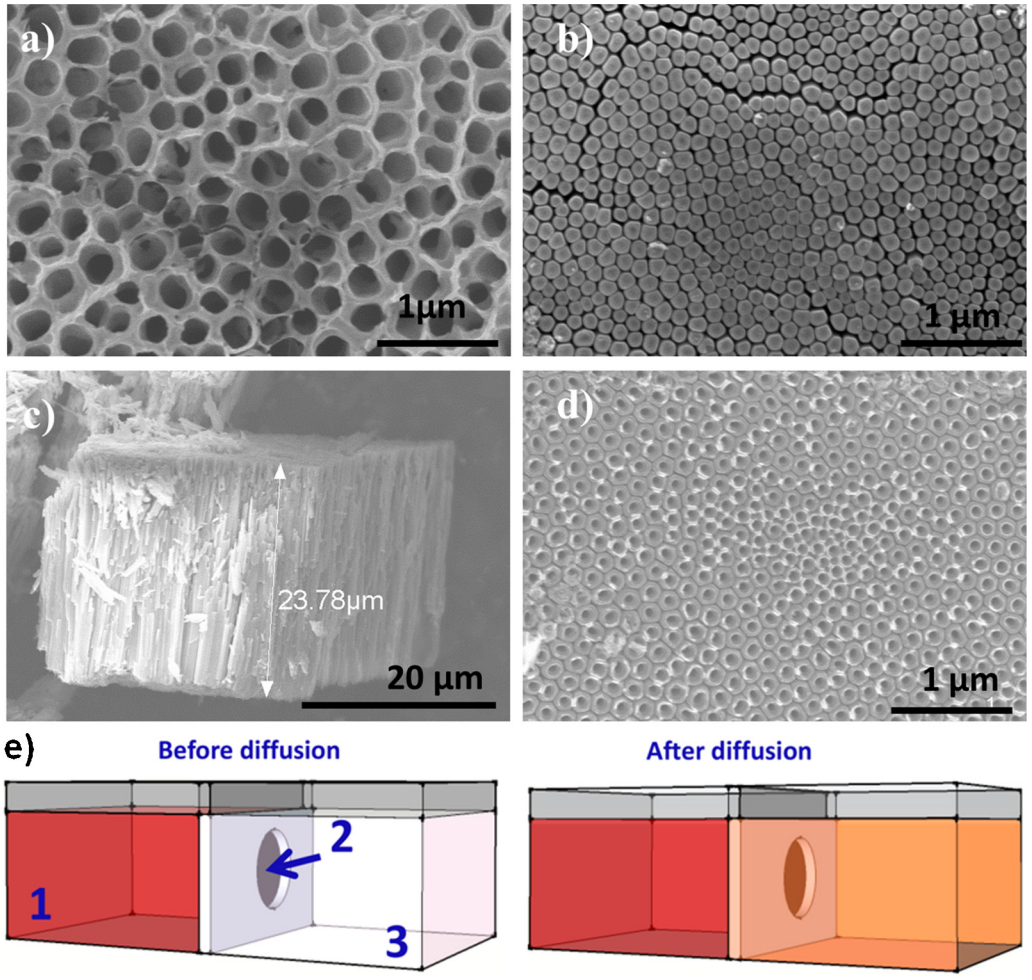

Fig. 1. SEM images of: a) top view of the membrane, b) closed bottom view of TiO_2 nanotubes, c) thickness of the membrane, d) bottom open view of membrane; e) schematic representation of the setup used for flow-through experiments (1. chamber containing AO7, 2. the TiO_2 membrane is glued on a holder with an opening, 3. chamber without AO7).

2.2. Membrane characterization

The morphology of the membrane was investigated using a scanning electron microscope (SEM) Hitachi FE-SEM 4800. The composition and the chemical states were characterized using X-ray photoelectron spectroscopy (XPS, PHI 5600, US), XPS spectra were acquired using an Al standard X-ray source with a pass energy of 23.5 eV and peak positions were calibrated on the Ti2p peak at 458.0 eV.

2.3. AO7 diffusion measurements

In order to investigate the permeability of the membranes, the membranes were mounted on a PVC holder. For this, the round membranes of 1 cm diameter were glued along their perimeter on a 0.5 cm diameter opening in the holder using epoxy resin. The holder was then placed as a separator wall in a two-compartment cell as shown in Fig. 1e. A series of experiments was performed using a 5×10^{-9} M Acid orange 7 (AO7) solution. The permeation of AO7 was evaluated by spectrophotometric measurements, using a UV/Vis spectrophotometer (Lambda XLS+, PerkinElmer) at λ=487 nm.

2.4. Feed solution

As background electrolyte three different types of ions were evaluated: 1) perchlorate, 2) phosphate, and 3) benzoate. The feed solution of perchlorate was prepared by using 0.05 M and 1 M lithium perchlorate in water-methanol (1:1) solution, while for phosphate and benzoate, 0.05 M potassium phosphate and potassium benzoate were used in a water-methanol (1:1) solution, respectively. pH adjustment was performed by using either perchloric acid or potassium hydroxide solutions.

2.5. Procedure of diffusion measurement

The experiments were carried out by filling the two compartments with the same amount of solutions (6 ml) and letting the membrane to be wetted for 5 hours. Then, AO7 was added to one of the compartments and stirred constantly. Every 30 minutes 2 ml of the solution in the other compartment was taken out and the absorption of the solution was measured by using a Lambda XLS–Perkin Elmer UV/Vis spectrophotometer measuring in the intensity of the dye main absorption band (λ = 487 nm), then the removal solution was returned to the compartment it was taken from.

2.6. Simulations

The spatial dependences of number density of ions and electric potential in the electrolyte solution and in contact with the charged TiO_2 surface were calculated by using an established mean-field lattice model of the electric double layer [20], which simultaneously takes into account the decrease of relative permittivity near the charged TiO_2 surface due to the orientational ordering of water dipoles, the excluded volume effect and the asymmetry of the anion and cation sizes. Accordingly, in our model electric double layer the hydrated positive and negative ions occupy α_+ and α_- lattice sites, respectively, while the water (solvent) molecule is assumed to occupy only one lattice site [15,20]:

$$n_s = \alpha_+ n_+(x) + \alpha_- n_-(x) + n_w(x) \quad (1)$$

Where $n_+(x)$, $n_-(x)$ and $n_w(x)$ are the number densities of cations, anions and water molecules, while n_s is the number density of lattice sites. In the bulk [20]:

$$n_s = \alpha_+ n_0 + \alpha_- n_0 + n_{0w} \quad (2)$$

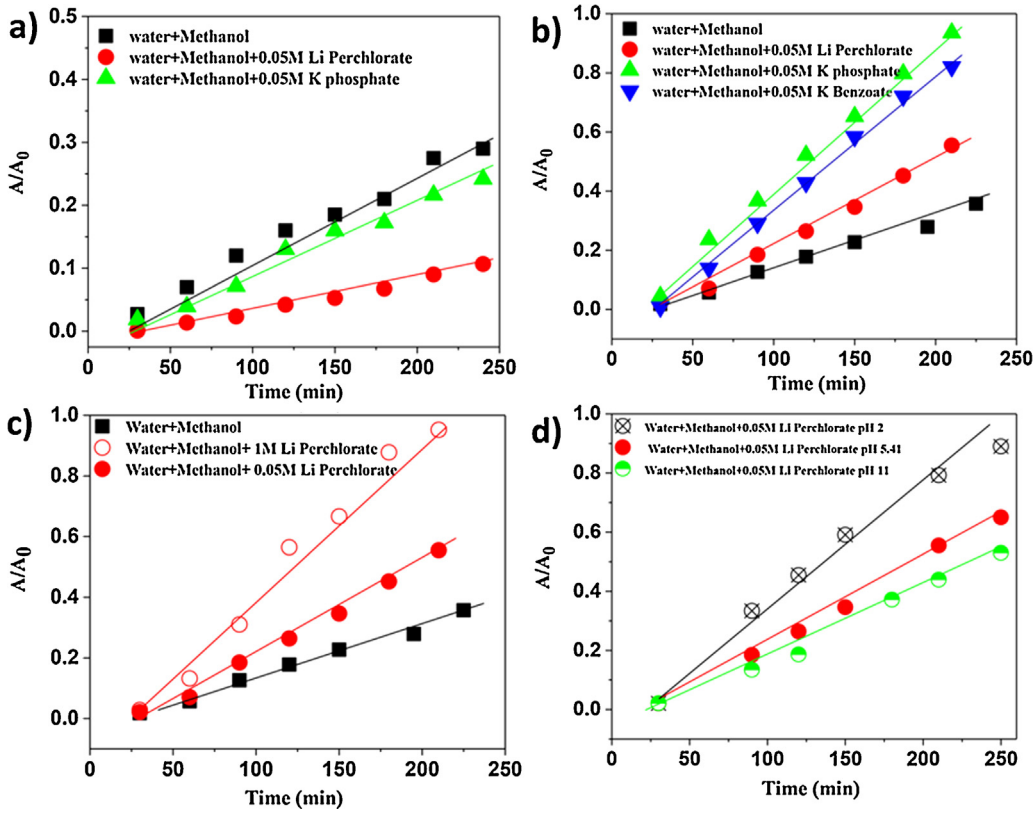

Fig. 2. Evaluation of AO7 permeation through the membrane: a) before wetting, b) effect of pre-wetting and ionic size, c) effect of ionic concentration, and d) effect of pH. Measurements were always performed in the non AO7-containing compartment of the cell.

where n_0 is the bulk number density of anions and cations and $n_{0w}/N_A = 55\ mol/l$ is the bulk number density of water molecules. The distance of closest approach at the outer Helmholtz plane is approximately equal to the hydration radius of the counter ions and is taken into account in our model of EDL as described in [15]. We assumed that there are no ions, but only water molecules in the Stern layer. The model equations were solved numerically using COMSOL Multiphysics® v.5.2a. software (COMSOL AB, Stockholm, Sweden) and considering the adequate boundary conditions [15]. The parameters used in the simulations are as following: the bulk concentration of ions $n_0/N_A = 0.05$ mol/l, dipole moment of water $p_0 = 3.1$ D, optical refractive index of water $n = 1.33$, relative size of negative ions $\alpha_- = 10$ and N_A is the Avogadro number.

3. Results and discussion

Electrochemical anodization of Ti under self-organizing conditions leads to the formation of TiO_2 nanotube arrays. In the present work, TiO_2 nanotubes are obtained by anodization at 120 V for 10 min at 60 °C, in an ethylene glycol (EG) electrolyte containing 1.5 M lactic acid (LA, DL-lactic acid, 90%, Fluka), 0.1 M ammonium fluoride (NH_4F), and 5 wt% deionized H_2O. The TiO_2 nanotube membranes are obtained by a simple re-anodization approach, as described in the experimental section and in [9]. For obtaining fast-growth long TiO_2 nanotubes, lactic acid (LA) is used as an additive, and in these conditions high voltages can be used without any oxide breakdown or severe tube damage [21].

Fig. 1a shows that the nanotubes are covered with a porous initiation layer, which is typical for EG based nanotubes, and show a good long-range order (due to the pre-anodization of the Ti foil, which effectively imprints the Ti foil with ordered concaves) [22,23]. The thickness of the nanotube membranes produced in this work is ca. 23 μm (Fig. 1c). The bottom view SEM images of the TiO_2 nanotubes and of the detached membrane are shown in Fig. 1b, d respectively, and confirm the open bottom structure of the membrane. To note, that usually nanotubes grown in organic electrolytes have the inner diameter at the bottom smaller than at the top (V-shape) [23].

To evaluate the flow-through properties of such TiO_2 nanotube membranes, we used AO7 as model marker (AO7 is also a classic model pollutant used in photocatalytic activity tests). It should be noted that AO7 may aggregate to small complexes, depending on the AO7 concentration in the solution [18]. Earlier experimental results indicated that the aggregation process may be affected greatly by the nature of the electrolyte [18]. As a consequence, factors such as screening effects of the salt ions [18] and/or short range attractive interaction between negatively charged AO7 (mediated by positively charged ions of electrolyte solution) [24], [25] play a crucial role. In this work the concentration of AO7 was selected to be low enough so that the mean aggregation number of AO7 can be assumed to be one [18].

The AO7 permeation through the TiO_2 nanotube membrane without any additional ions as well as in the presence of lithium perchlorate and potassium phosphate is shown in Fig. 2. In Fig. 2a and 2b membranes were used either “dry” or after a 5 hours pre-wetting of the membrane in the background electrolyte. In the dry state, clearly the background ion free solution permeates the fastest. This is in stark contrast to the pre-wetted membrane in Fig. 2b. The decreased permeation due to foreign ions addition may likely be ascribed to capillary effects [26]. Moreover,

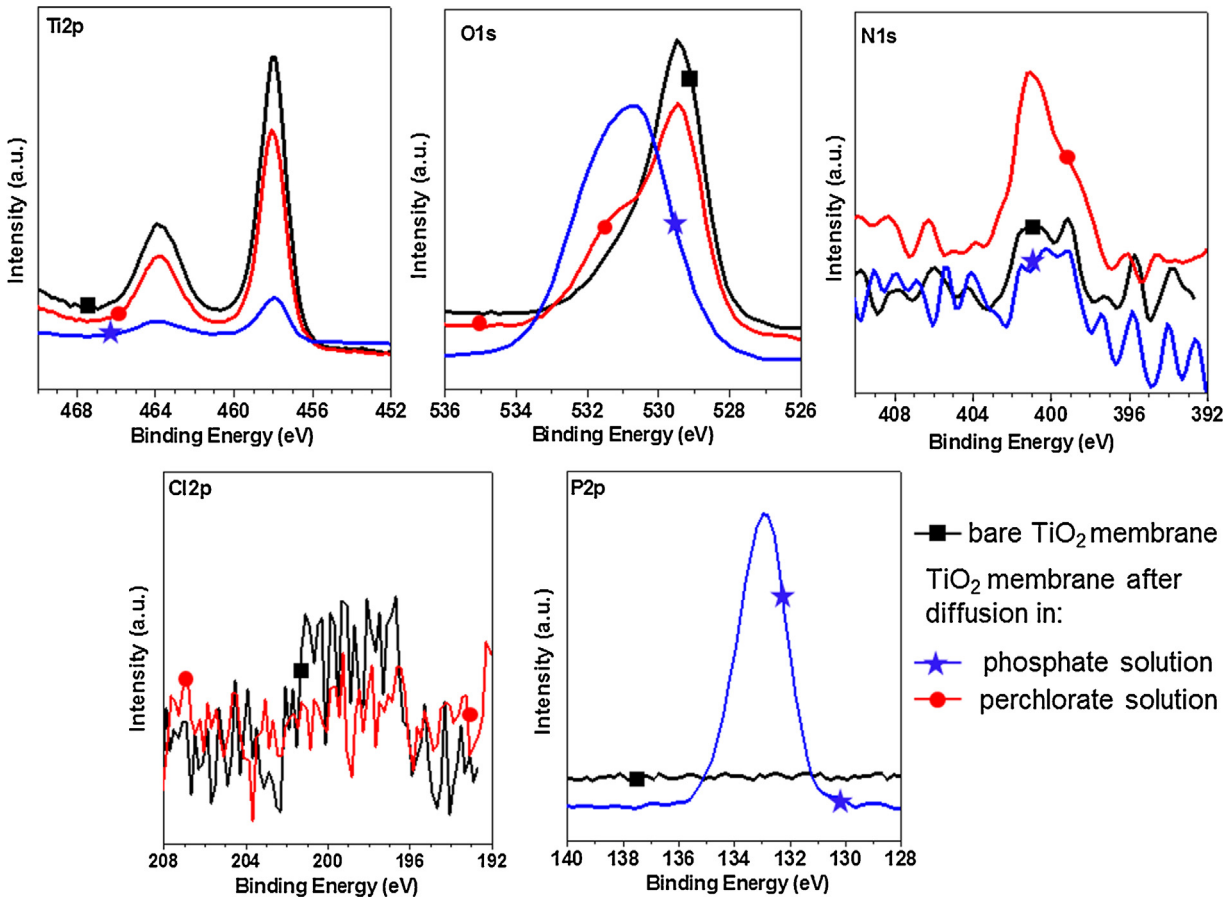

Fig. 3. High resolution XPS spectra of the bare membrane (black square) and of the membranes after diffusion tests in phosphate (blue star) and perchlorate (red circle) solutions.

measurements with pre-wetted membranes show less experimental scatter and allow electrolyte ions to reach adsorption equilibrium with the TiO_2 nanotube walls.

3.1. Pre-wetting and ionic size effect

Using a 5 hours wetting was found to give stable reproducible results - the effect of wetting is illustrated in Fig. 2b. While for the plain water-methanol mixture the AO7 diffusion is only slightly higher than in Fig. 2a, for all other solutions containing additional ions, after 5 h wetting the AO7 diffusion rates and thus the permeability of the membranes become much higher with the addition of background ions. Pre-wetting for 5 hours allows a full wetting of the membrane, which ensures that the inner surface becomes completely stable with regard to its electric charge (adsorption/chemisorption of ions). Note that the zeta potential values of the inner surface of TiO_2 nanotubes become less negative with an increase in ion concentration [15].

When using different ions in similar concentration (Fig. 2b), we observe that the electrolytes containing potassium benzoate or potassium phosphate allow for a higher amount of AO7 passing through, as compared to the lithium perchlorate containing electrolyte. This result can be partially explained by the larger hydrated radius of lithium in comparison to the size of potassium hydrated radius and the consequent different hydrodynamic radii of AO7 molecules surrounded by the cloud electrical double layer (EDL) of hydrated K^+ counter ions in potassium benzoate solution and AO7 molecules surrounded by the cloud (EDL) of hydrated Li^+ counter ions in lithium perchlorate solution. Namely, this means that the larger hydrated counter ions produce more extended (thicker) EDL, as indicated by the theoretical simulations of the electric double layer – see Fig. 4.

It is well established that potassium is weakly hydrated with only a single shell of water molecules, while the smaller lithium ion is more strongly hydrated with a second hydration shell [27]. In accordance, the ionic mobility of Li^+ is about two times smaller than the mobilities of K^+ ions [28], meaning that the hydrodynamic radius (radius of the hydrated ion) of Li^+ is larger than that of K^+. The mobility of the weakly hydrated Cl^- ions is very similar to that of K^+ ions [28].

The diffusion coefficient depends on the size of the molecule, i.e. larger molecules diffuse slower than smaller molecules. Due to this counter ion effect the diffusion rate of AO7 is therefore expected to be smaller in lithium perchlorate than in potassium phosphate solution.

Additionally, in order to study adsorption of ions on TiO_2, we investigated a membrane in XPS after permeation experiments in the presence of phosphate and perchlorate ions and AO7 (see Fig. 3). Compared to the nanotube membrane in water-methanol permeation experiments, in the presence of phosphate ions we observe a decrease in the Ti2p peak, a shift in the O1s peak (due to the decrease of the O1s signal corresponding to TiO_2 and increase of the O1s from the phosphate) and the presence of P2p. Moreover, for phosphate solution we observe similar N1s peaks before and after permeation, which is attributed to nitrogen pick-up from the atmosphere, thus no AO7 adsorption could be detected. The finding of a stable phosphate adsorption layer suggests that adsorption/chemisorption of phosphate ions to the inner surfaces of TiO_2 nanotubes makes this surface more negatively charged. This adsorbed negative surface electric potential (see Fig. 4d) changes the wetting properties [26] and the boundary slip flow [29]. Both phenomena can contribute to the modified permeation of AO7 through the TiO_2 nanotube membrane. On the other hand, for the membrane in the presence of perchlorate ions, no perchlorate adsorption on the TiO_2 nanotube membrane was

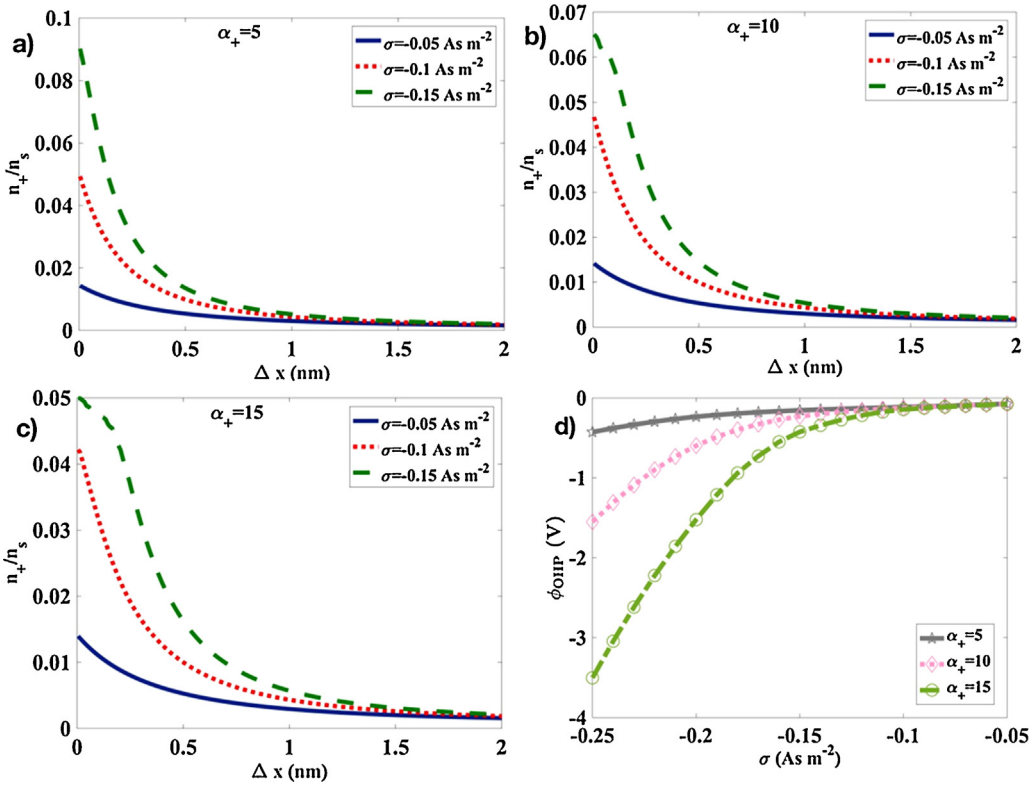

Fig. 4. Evaluation at the outer Helmholtz plane (OHP) of the charged TiO_2 surface for the relative number density of positive ions $n_+(x)/n_s$ as a function of the distance (Δx) from the OHP for three different values of the relative size of the positively charged monovalent counterions α_+: a) $\alpha_+ = 5$, b) $\alpha_+ = 10$ and c) $\alpha_+ = 15$ and d) the electric potential at OHP as a function of the negative TiO_2 surface charge density σ for various α_+.

observed. Nevertheless, for perchlorate solution a small N1s peak is observed, as well as a shoulder in the O1s peak (corresponding to –OH bonds, at 531.5 eV). The presence of the N1s peak after permeation can be attributed to AO7 fouling, which confirms the results in Fig. 2b.

3.2. Effect of electrolyte concentration and pH

In order to investigate the effect of ion concentration on the permeation of AO7, lithium perchlorate ($LiClO_4$) was chosen as its concentration can be adjusted to higher values. Fig. 2c shows the permeation of AO7 without and with additions of 0.05 M $LiClO_4$ and 1 M $LiClO_4$. Clearly, with a higher concentration of $LiClO_4$ AO7 passes through the membrane faster.

In literature, experimental and theoretical results for other oxide membranes show that the distance from the charged surface to the hydrodynamic slip/shear plane is decreasing with increasing salt concentration [15]. In accordance, also in our case of AO7 ions, for higher background ion salt concentrations, hydrodynamic radius of the AO7 ions in higher concentration of background ions is smaller than in low concentration solutions, which causes the faster permeation of AO7 through the TiO_2 nanotube membrane. In agreement, the results presented in Fig. 2c show faster and more efficient permeation of AO7 at higher salt concentrations.

It is worth mentioning that TiO_2 nanotubes have an IEP at a pH value of around 4.2-5.1, depending on the nanotubes' diameter and type of anodization electrolyte [15], meaning that at pH values higher than these, the TiO_2 surface is negatively charged. Namely, when the membrane surface comes into contact with the electrolyte solution, ions in the electrolyte rearrange according to charge, to screen the charge of TiO_2, and thus alter the electrical double layer (EDL). According to the classical Gouy-Chapman-Stern model, the EDL can be characterized by the surface potential, EDL thickness and the zeta potential [30]. Fig. 4 shows the modeling of electrostatic interactions, the space dependence of the number density of ions near the TiO_2 surface, and the space dependence of the electric potential seems to be more important than the surface charged density of TiO_2 surface itself.

By increasing the ion concentration, both the thickness of EDL (Eq.1) and the magnitude of the zeta potential decrease in magnitude (correspondingly the electric potential at the outer Helmholtz plane is decreased) [15,30]. With increasing electrolyte concentration, the surface charge is therefore screened/compensated already at a lower distance from the TiO_2 surface, which means that the magnitude of the potential drops faster and the thickness of EDL decreases significantly [15,30]. The hydrated ionic radius of the salt counter ions determines its maximum possible concentration at the TiO_2 charged surface [20,31]. Larger hydrated salt counter ions produce more negative electric potential at the charged surface, as shown in Fig. 4d, and a more extended (i.e. thicker) EDL as indicated in Fig. 4a, b, c, in accordance with the results of some previous studies [27,30,32].

If the pH of the solution is above the IEP of TiO_2, increasing the salt concentration amplifies the shielding of the negative electric charge of the nanotube surface inside the TiO_2 nanotubes, which can then reduce the strong repulsive forces toward AO7. If the pH is below the IEP of TiO_2, the inner surface of TiO_2 nanotubes is positively charged and an increased salt concentration reduces the attraction forces between the positively charged inner nanotube surface and the negatively charged AO7. As the pH of the solution has thus a significant effect on the surface charge of the TiO_2 membrane [15], we further investigated the permeate flux of AO7 solution through the TiO_2 membrane at a fixed concentration of salt (i.e. 0.05 M $LiClO_4$) and at different pH values (see Fig. 2d). We observe that the permeate flux of AO7 increases at lower pH values.

Variation of pH changes the surface charge density of the inner surface of TiO_2 nanotubes. At a lower pH such as 2, when the TiO_2 nanotubes are positively charged, ClO_4^- ions are predominant in the diffuse layer near the inner surface of nanotubes. ClO_4^- ions have smaller hydrodynamic radius compared to the Li^+ [33]. Shielding of the positively charged inner surface of the TiO_2 nanotubes with ClO_4^- ions thus reduces the attractive force between AO7 and the inner surface TiO_2 nanotubes, and this is a likely origin for the facilitated passing of the negatively charged AO7 through the TiO_2 nanotubes of the membrane.

On the other hand, at a pH higher than the isoelectric point of TiO_2, the membrane walls are negatively charged, therefore Li^+ ions screen the negatively charged TiO_2 surface and partially also adsorb on the TiO_2 surface. The screening of the electrostatic field by the Li^+ counter ions that accumulate near the negatively charged TiO_2 surface can be described by the effective thickness of the electrical double layer.

3.3. Modeling

In order to estimate the charge distribution and take into account the different values of the relative size of the positively charged monovalent counter ions and the electric potential at outer Helmholtz plane as a function of the negative TiO_2 surface charge density, we use a model previously developed [33,35].

In previous works we have introduced the distance $x_{1/2}$, where the density of the number of the counter ions (calculated relative to its value far from the charged surface) drops to half of its value at the charged surface. Within the Gouy-Chapman model the effective thickness of EDL $x_{1/2}$ can be expressed as [33,35]:

$$x_{1/2} = \frac{1}{\kappa}\ln\left(\frac{\left(\sqrt{1+\exp(-e_0\phi_0/kT)/2}+1\right)\left(1-\exp(-e_0\phi_0/2kT)\right)}{\left(\sqrt{1+\exp(-e_0\phi_0/kT)/2}-1\right)\left(1+\exp(-e_0\phi_0/2kT)\right)}\right) \quad (3)$$

where $1/\kappa = \sqrt{\varepsilon_r\varepsilon_0 kT/2n_0e_0^2}$ is the Debye length, e_0 is the unit charge, kT is the thermal energy and the surface electric potential: $\phi_0 = -(2kT/e_0)\ln\left(\sqrt{1+(\sigma/c)^2}+||\sigma|)/c\right)$. Here $c = \sqrt{8kT\varepsilon_r\varepsilon_0 n_0}$, n_0 is the bulk number density of salt ions (i.e. the number density at the center of the nanotubes), ε_0 is the permittivity of the free space and ε_r is the relative permittivity of the solution. For small n_0, the value of c is small and σ/c is large, leading to the following limit expression of Eq. (3):

$$x_{1/2} \cong \frac{2\varepsilon_r\varepsilon_0 kT}{e_0||\sigma|)}\left(\sqrt{2}-1\right) \quad (4)$$

Eq. (3) is valid for not too large values of the surface charge $||\sigma|)$ [34,35] and indicates that a more negative TiO_2 surface (due to a pH increase) attracts in its vicinity larger number of Li^+ ions. Thus the screening is more effective and EDL effective thickness $x_{1/2}$ is diminished as shown in Eq. (4). The monotonous decreasing $x_{1/2}$ with increasing $||\sigma|)$ can be observed also in Fig. 4, but this holds only for a sufficiently small size of the counter ions, i.e. for $\alpha_+ = 5$ and $\alpha_+ = 10$ (Fig. 4a, b).

With increasing $||\sigma|)$ at still higher pH more Li^+ ions are attracted to EDL at the inner surface (i.e. at OHP) of the TiO_2 nanotubes. However, for large hydrated Li^+ ions the excluded volume effect imposes an upper limit on the density of the number of Li^+ counter ions near the charged TiO_2 surface where Li^+ counter ions are accumulated. This phenomenon can be seen in Fig. 4, where the number density of counter ions $n_+(x)$ for larger values of $||\sigma|)$ starts to saturate at small distances (Δx) from the OHP plane (see Fig. 4c). This saturation effect can be observed only for large

enough size of counter ions (i.e. for $\alpha_+ = 15$ and very weakly also for $\alpha_+ = 10$, but not for $\alpha_+ = 5$) and for large enough value of $||\sigma|| = 0.15\ As/m^2$ (see Fig. 4c). Namely, the influence of the excluded volume effect increases with increasing $||\sigma||$ (driven by increasing pH), so that $x_{1/2}$ after reaching its minimal value, begins to increase with increasing $||\sigma||$ which can be seen in Fig. 4c for the case $\alpha_+ = 15$. In addition, adsorption/chemisorption of salt ions might be increased as well due to pH induced change of the surface charged density of the inner surface of TiO_2 nanotubes.

Both above described effects of pH may change the TiO_2 nanotube wetting properties [26] and the boundary slip flow [29] at the inner TiO_2 nanotube wall surface and decrease the permeation of AO7 molecules through TiO_2 nanotubular membrane as experimentally observed in Fig. 2d.

In addition, at larger pH values the AO7 molecules might also be more negatively charged, therefore the thickness of the EDL around the single AO7 particle (i.e. the corona composed of large hydrated Li^+ counter ions and water molecules) becomes increased, as indicated in Fig. 4c. Hence, the hydrodynamic radius of AO7 is also larger, and therefore the diffusion coefficient of AO7 is decreased.

4. Conclusions

The present work shows that the flux of a marker dye (AO7) through a free standing TiO_2 nanotube membrane is significantly affected by electrokinetic properties of the membrane surface, which is among others related to the ionic strength and pH of the feed solution. Results revealed that at lower pH values than the isoelectric point, more AO7 permeation can be seen through the TiO_2 membrane. Furthermore, by increasing the concentration of salt in the electrolyte, the diffusion rate is improved as well. These changes may be attributed to the changes of the TiO_2 surface charge density (σ) and the resulting changes in EDL at the TiO_2 surface which influence the wetting properties of the inner surface of TiO_2 nanotubes and the boundary slip flow in the nanotubes.

The influence of the size of the salt ions on the permeation of AO7 through the TiO_2 nanotube membrane was also studied by using Li^+ ions, which have larger hydrated ionic diameter compared with K^+ ions. Experimental results and modeling show that the size of the salt ions has a considerable impact on the permeation of AO7, due to the different hydrodynamic radius of AO7 molecules (i.e. the radius of the naked AO7 ion together with the surrounding layer of salt counter ions and water molecules). The smaller the hydrodynamic radius of AO7, the higher is the permeation of AO7 through the TiO_2 nanotube membrane.

Acknowledgements

The authors would like to acknowledge the ERC, the DFG, the DFG “Engineering of Advanced Materials” cluster of excellence and ARRS for financial support.

References

[1] P. Roy, S. Berger, P. Schmuki, TiO_2 nanotubes: Synthesis and applications, Angew. Chemie - Int. Ed. 50 (2011) 2904–2939.
[2] Z.R. Hesabi, N.K. Allam, K. Dahmen, H. Garmestani, M.A. El-Sayed, Self-standing crystalline TiO_2 nanotubes/CNTs heterojunction membrane: Synthesis and characterization, ACS Appl. Mater. Interfaces. 3 (2011) 952–955.
[3] H. Zhang, X. Quan, S. Chen, H. Zhao, Y. Zhao, Fabrication of photocatalytic membrane and evaluation its efficiency in removal of organic pollutants from water, Sep. Purif. Technol. 50 (2006) 147–155.
[4] O. Benhabiles, H. Mahmoudi, H. Lounici, M.F.A. Goosen, Effectiveness of a photocatalytic organic membrane for solar degradation of methylene blue pollutant, Desalin. Water Treat. 57 (2016) 14067–14076.
[5] P. Roy, T. Dey, K. Lee, D. Kim, B. Fabry, P. Schmuki, Size-selective separation of macromolecules by nanochannel titania membrane with self-cleaning (Declogging) ability, J. Am. Chem. Soc. 132 (2010) 7893–7895.
[6] Q. Zhang, Y. Fan, N. Xu, Effect of the surface properties on filtration performance of Al_2O_3-TiO_2 composite membrane, Sep. Purif. Technol. 66 (2009) 306–312.
[7] J.K. Pi, H.C. Yang, L.S. Wan, J. Wu, Z.K. Xu, Polypropylene microfiltration membranes modified with TiO_2 nanoparticles for surface wettability and antifouling property, J. Memb. Sci. 500 (2016) 8–15.
[8] I. Kumakiri, S. Diplas, C. Simon, P. Nowak, Photocatalytic membrane contactors for water treatment, Ind. Eng. Chem. Res. 50 (2011) 6000–6008.
[9] S.P. Albu, A. Ghicov, J.M. Macak, R. Hahn, P. Schmuki, Nanotube Membrane for Flow-through Photocatalytic Applications, (2007) , pp. 5–8.
[10] F. Mohammadpour, M. Moradi, K. Lee, G. Cha, S. So, A. Kahnt, D.M. Guldi, M. Altomare, P. Schmuki, Enhanced performance of dye-sensitized solar cells based on TiO_2 nanotube membranes using an optimized annealing profile, Chem. Commun. 51 (2015) 1631–1634.
[11] F. Mohammadpour, M. Altomare, S. So, K. Lee, M. Mokhtar, A. Alshehri, S.A.A. Thabaiti, P. Schmuki, High-temperature annealing of TiO_2 nanotube membranes for efficient dye-sensitized solar cells, Semicond. Sci. Technol. 31 (2016) 014010.
[12] P. Wu, Y. Xu, Z. Huang, J. Zhang, Processing Research A review of preparation techniques of porous ceramic membranes, Ceram. Process. Res. 16 (2015) 102–106.
[13] L.Y. Ng, A.W. Mohammad, C.P. Leo, N. Hilal, Polymeric membranes incorporated with metal/metal oxide nanoparticles: A comprehensive review, Desalination. 308 (2013) 15–33.
[14] F.F. Nazzal, M.R. Wiesnef, MEE2E membranes in water filtration, (1994) 7388.
[15] M. Lorenzetti, E. Gongadze, M. Kulkarni, I. Junkar, A. Iglič, Electrokinetic Properties of TiO_2 Nanotubular Surfaces, Nanoscale Res. Lett. 11 (2016) 378.
[16] F.L. Hua, Y.F. Tsang, Y.J. Wang, S.Y. Chan, H. Chua, S.N. Sin, Performance study of ceramic microfiltration membrane for oily wastewater treatment, Chem. Eng. J. 128 (2007) 169–175.
[17] Q. Zhang, Y. Fan, N. Xu, Effect of the surface properties on filtration performance of Al2O3–TiO2 composite membrane, Sep. Purif. Technol. 66 (2009) 306–312.
[18] S. Bračko, J. Špan, Osmotic coefficients of C.I. Acid Orange 7 in aqueous solution and in the presence of simple electrolyte, Dye. Pigment. 35 (1997) 165–169.
[19] L. Bulavin, Specific Features of Motion of Cations and Anions in Electrolyte Solutions, (2011) .
[20] E. Gongadze, A. Iglič, Asymmetric size of ions and orientational ordering of water dipoles in electric double layer model - an analytical mean-field approach, Electrochim. Acta. 178 (2015) 541–545.
[21] S. So, K. Lee, P. Schmuki, Ultrafast growth of highly ordered anodic TiO_2 nanotubes in lactic acid electrolytes, J. Am. Chem. Soc. 134 (2012) 11316–11318.
[22] F. Mohammadpour, M. Moradi, G. Cha, S. So, K. Lee, P. Schmuki, A Comparison of Anodic TiO_2 Nanotube Membranes used for Front-side Illuminated Dye-Sensitized Solar Cells, Chemelctrochem. 2 (2015) 204–207.
[23] K. Lee, A. Mazare, P. Schmuki, One-dimensional titanium dioxide nanomaterials: Nanotubes, Chem. Rev. 114 (2014) 9385–9454.
[24] J. Zelko, V. Kralj-Iglič, P.B.S. Kumar, J. Zelko, A. Iglič,, Effects of counterion size on the attraction between similarly charged surfaces, J. Chem. Phys 133 (2010).
[25] J. Urbanija, K. Bohinc, A. Bellen, S. Maset, V. Kralj-, P.B. Sunil, J. Urbanija, K. Bohinc, A. Bellen, S. Maset, A. Iglič, V. Kralj-Iglič, P.B.S. Kumar, Attraction between negatively charged surfaces mediated by spherical counterions with quadrupolar charge distribution, J. Chem. Phys. 129 (2008) 105101-1–105101-5.
[26] J. Berthier, K.A. Brakke, Capillary Effects: Capillary Rise, Capillary Pumping, and Capillary Valve, in: Phys. Microdroplets, John Wiley & Sons, Inc, 2012, pp. 183–208.
[27] J. Mähler, I. Persson, A Study of the Hydration of the Alkali Metal Ions in Aqueous Solution, Inorg. Chem. 51 (2012) 425–438.
[28] P.R. Bergethon, The Physical basis of biochemistry, 2nd edition, Springer, 2010.
[29] H. Huang, Z. Song, N. Wei, L. Shi, Y. Mao, Y. Ying, L. Sun, Z. Xu, X. Peng, Ultrafast viscous water flow through nanostrand-channelled graphene oxide membranes, Nat. Commun. 4 (2013) 2979.
[30] M.A. Brown, A. Goel, Z. Abbas, Effect of electrolyte concentration on the Stern Layer thickness at a charged interface, Angew. Chemie. 55 (2016) 3790–3794.
[31] Y. Yukselen-Aksoy, A. Kaya, A study of factors affecting on the zeta potential of kaolinite and quartz powder, Environ. Earth Sci. 62 (2011) 697–705.
[32] C.N. Patra, L.B. Bhuiyan, The effect of ionic size on polyion-small ion distributions in a cylindrical double layer, Condens. Matter Phys. 8 (2005) 425–446.
[33] J. Buffle, Z. Zhang, K. Startchev, Metal Flux and Dynamic Speciation at bio interfaces. Part I: Critical Evaluation and Compilation of Physicochemical Parameters for Complexes with Simple Ligands and Fulvic/Humic Substances, Environ. Sci. Technol. 41 (2007) 7609–7620.
[34] V. Kralj-Iglič, A. Iglič, A Simple Statistical Mechanical Approach to the free Energy of the Electric Double Layer Including the Excluded Volume Effect, J. Phys. II Fr. 6 (1996) 477–491.
[35] K. Bohinc, V. Kralj-Iglič, A. Iglič, Thickness of electrical double layer. Effect of ion size, Electrochim. Acta. 46 (2001) 3033–3040.